American Mineralogist, Volume 104, pages 1356–1359, 2019

LETTER

The stability of Fe_5O_6 and Fe_4O_5 at high pressure and temperature

KOUTARO HIKOSAKA[1,*,†], RYOSUKE SINMYO[1], KEI HIROSE[1,2], TAKAYUKI ISHII[3], AND YASUO OHISHI[4]

[1]Department of Earth and Planetary Science, Graduate School of Science, The University of Tokyo, 7-3-1 Hongo, Bunkyo, Tokyo 113-0033, Japan
[2]Earth-Life Science Institute, Tokyo Institute of Technology, 2-12-1 Ookayama, Meguro, Tokyo 152-8550, Japan
[3]Bayerisches Geoinstitut, Universität Bayreuth, D-95440 Bayreuth, Germany. Orcid 0000-0002-1494-2141
[4]Japan Synchrotron Radiation Research Institute, 1-1-1 Koto, Sayo, Hyogo 679-5198, Japan

ABSTRACT

The oxygen fugacity in the interior of the Earth is largely controlled by iron-bearing minerals. Recent studies have reported various iron oxides with chemical compositions between FeO and Fe_3O_4 above ~10 GPa. However, the stabilities of these high-pressure iron oxides remain mostly uninvestigated. In this study, we performed in situ X-ray diffraction (XRD) measurements in a laser-heated diamond-anvil cell (DAC) to determine the phase relations in both Fe_5O_6 and Fe_4O_5 bulk compositions to 61 GPa and to 2720 K. The results show that Fe_5O_6 is a high-temperature phase stable above 1600 K and ~10 GPa, while FeO + Fe_4O_5 are formed at relatively low temperatures. We observed the decomposition of Fe_5O_6 into 2FeO + Fe_3O_4 above 38 GPa and the decomposition of Fe_4O_5 into FeO + h-Fe_3O_4 at a similar pressure range. The coexistence of FeO and Fe_3O_4 indicates that none of the recently discovered compounds between FeO and Fe_3O_4 (i.e., Fe_5O_6, Fe_9O_{11}, Fe_4O_5, and Fe_7O_9) are formed beyond ~40 GPa at 1800 K, corresponding to conditions in the shallow lower mantle. Additionally, as some superdeep diamonds have genetic links with these high-pressure iron oxides, our results give constraints on pressure and temperature conditions of their formation.

Keywords: Iron oxide, diamond-anvil cell, high pressure, Fe_4O_5, Fe_5O_6; Volatile Elements in Differentiated Planetary Interiors

INTRODUCTION

Since iron is the most abundant transition metal element, oxygen fugacity inside the Earth is controlled by iron-bearing phases. According to recent analyses of natural samples, oxygen fugacity varies widely in the mantle (Kaminsky et al. 2015; Smith et al. 2016). Oxidizing materials include a fair amount of Fe^{3+}, which may stabilize iron oxides as discrete minerals. Recent high-pressure experimental studies have discovered a rich variety of iron oxides intermediate in composition between FeO and Fe_3O_4, including Fe_5O_6 (Lavina and Meng 2015), Fe_9O_{11} (Ishii et al. 2018), Fe_4O_5 (Lavina et al. 2011), and Fe_7O_9 (Sinmyo et al. 2016). However, the pressure-temperature (*P-T*) stability fields of these iron oxides are poorly known.

To understand the speciation of volatile elements in the mantle, mineral redox buffer relations have been revised considering these new iron oxides; for example, Myhill et al. (2016) showed that FeO-Fe_5O_6 line crosses the enstatite + magnesite = olivine + diamond (EMOD) buffer line, suggesting Fe_5O_6 is stable at conditions where diamonds are formed. Therefore, a better understanding of the thermodynamic stability of high-pressure, high-temperature iron oxides might enable a more refined understanding of the redox of the Earth's lower mantle and the origin of super-deep diamonds.

Here we examined the phase relations in Fe_5O_6 and Fe_4O_5 bulk compositions on the basis of high *P-T* experiments up to 61 GPa and to 2720 K. Our results demonstrate that the stabilities of Fe_5O_6 and Fe_4O_5 are limited to 35–40 GPa at 1800 K and both are decomposed into FeO wüstite + h-Fe_3O_4 at higher pressures. Furthermore, our findings indicate that no intermediate compounds between FeO and Fe_3O_4, including more recently discovered Fe_9O_{11} and Fe_7O_9, are formed above ~40 GPa.

METHODS

We used Fe_5O_6 and Fe_4O_5 as starting materials, both of which were synthesized from mixtures of reagent-grade Fe metal and Fe_2O_3 hematite powders at 10 GPa/1700 K and 15 GPa/1700 K, respectively, in a Kawai-type multi-anvil press at the Bayerisches Geoinstitut (Ishii et al. 2016). The Raman spectra of the Fe_5O_6 sample were collected at 1 bar and at high pressures to 27 GPa in a diamond-anvil cell (DAC) without any pressure medium by using a micro-confocal laser Raman system (JASCO NRS-3100) (Supplemental[1] Fig. S1).

Laser-heated DAC experiments were performed using diamond anvils with 300 μm culets. The Fe_5O_6 and Fe_4O_5 samples were pressed into ~10 μm thick plates and loaded into 100 μm sample chambers at the centers of pre-indented rhenium gaskets. NaCl or KCl, dried in an oven until just prior to the loading, was used as both a pressure medium and a pressure standard. After compression, the sample was heated from both sides using 100 W single-mode Yb fiber lasers with beam-shaping optics, which converts a Gaussian beam to one with a flat energy distribution. Using this flat-top laser heating system, the resultant laser-heated spots had reduced radial temperature gradients and were approximately 30 μm in diameter. We measured temperature using spectroradiometry (Ozawa et al. 2016). Sample pressures were calculated from the unit-cell volume of NaCl-B1 (Brown 1999), NaCl-B2 (Ueda et al. 2008), or KCl (Dewaele et al. 2012) at high *P-T* obtained by X-ray diffraction (XRD) measurements. The temperatures of NaCl and KCl were estimated from measured sample temperature (T_{meas}) (Pigott et al. 2015) as;

* E-mail: hikosaka@g.ecc.u-tokyo.ac.jp
† Special collection papers can be found online at http://www.minsocam.org/MSA/AmMin/special-collections.html.

0003-004X/19/0009–1356$05.00/DOI: https://doi.org/10.2138/am-2019-7097

$$T_{\mathrm{NaCl,KCl}} = \frac{3T_{\mathrm{meas}} + 300}{4} \pm \frac{T_{\mathrm{meas}} - 300}{4} \quad (1)$$

In situ XRD measurements were conducted at the BL10XU, SPring-8. An incident X-ray beam with a wavelength of 0.4127–0.4158 Å was focused using compound refractive lenses and collimated so that the full-width at half maximum was 6 μm. XRD patterns were collected on a flat panel detector (Perkin Elmer) with an exposure time of 1 s during heating and 20–30 s at 300 K. We employed the IPAnalyzer software package to integrate the 2D diffraction patterns into 1D patterns and the PDIndexer to analyze the pattern.

RESULTS

Stability fields of Fe_5O_6 and Fe_4O_5

A total of nine separate high *P-T* runs were used to determine the phase relations in the Fe_5O_6 bulk composition (Fig. 1a). Since the Fe_5O_6 starting material consisted of a small number of grains and was under large deviatoric stress upon compression at room temperature, it exhibited broad and limited XRD peaks at high pressure before heating. Figures 2a and 2b show the changes in integrated XRD patterns for run 8 (see Supplemental[1] Fig. S2 for the raw 2D XRD images). All peaks from the sample were indexed to Fe_5O_6 before heating at 36 GPa. Upon heating to 1930 K, the peaks from Fe_5O_6 mostly disappeared, and new FeO wüstite and Fe_4O_5 peaks were observed. With further heating to 2350 K at 34 GPa, the peaks of Fe_5O_6 emerged once again in <1 min. This sample was compressed further to 59 GPa. At this point, the area outside the laser-heated spot had decomposed into FeO + Fe_4O_5 due to the temperature gradient. Soon after we started heating a new spot consisting of FeO + Fe_4O_5, the XRD pattern drastically changed, showing the presence of FeO wüstite + h-Fe_3O_4. While the crystal structure of h-Fe_3O_4 remains controversial, we assume its space group to be *Cmcm* based on Ricolleau and Fei (2016). On the basis of these experiments using Fe_5O_6 as the starting material, we found that the stability of Fe_5O_6 is limited to temperatures above 1500 K and a pressure range of 10 to 36 GPa (Fig. 1a). Furthermore, the boundary between Fe_5O_6 and FeO + Fe_4O_5 has a small positive Clapeyron slope. In the other runs, we heated a previously unheated portion of a sample at each heating cycle. The stabilities of Fe_5O_6, FeO + Fe_4O_5, and FeO + h-Fe_3O_4 in the Fe_5O_6 bulk composition were determined on the basis of the appearance of new diffraction peaks and their growth (Fig. 1a). The peaks from preexisting, unstable phase(s) decreased in intensity but did not fully disappear due to sluggish kinetics of phase transitions between these phases.

We have also conducted an additional experiment using Fe_4O_5 as a starting material (run no.12). Broad XRD peaks from Fe_4O_5 were present at 39 GPa and 300 K. They became sharp during heating up to 1620 K. With further heating to 1860 K and above, we observed the dissociation of Fe_4O_5 into FeO wüstite + h-Fe_3O_4 (Fig. 2c). The *P-T* stability of Fe_4O_5, in experiments using starting compositions of bulk Fe_4O_5 and Fe_5O_6 (through the decomposition of Fe_5O_6 at high temperatures), are shown in Figure 1b. Fe_4O_5 is stable as a single phase up to 38 GPa at 1950 K and ~60 GPa at 1200 K. The boundary between Fe_4O_5 and FeO + h-Fe_3O_4 exhibits a negative Clapeyron slope although the slope is not tightly constrained from the present experiments.

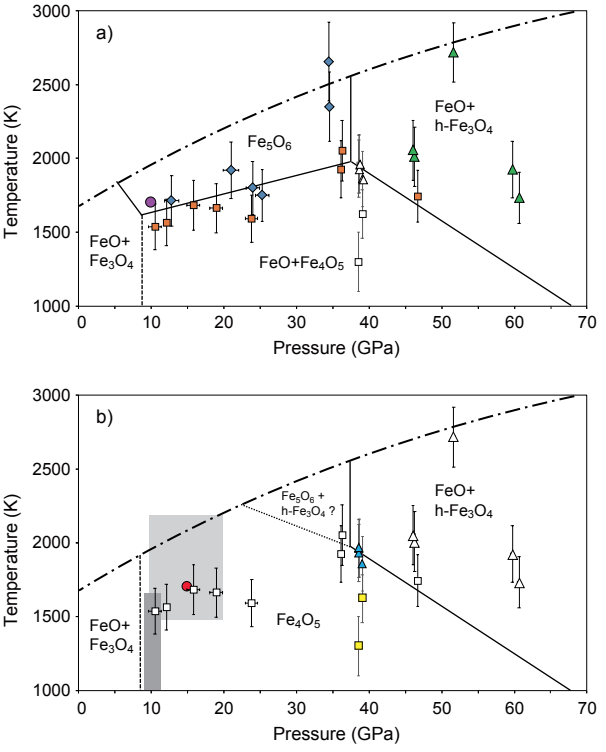

FIGURE 1. Phase relations in (**a**) Fe_5O_6 and (**b**) Fe_4O_5 bulk compositions. In **a**, blue diamonds = Fe_5O_6; orange squares = FeO + Fe_4O_5; green triangles = FeO + h-Fe_3O_4; purple circle = condition for synthesizing the Fe_5O_6 starting material. White squares and triangles are from **b**. In **b**, yellow squares = Fe_4O_5; light blue triangles = FeO + h-Fe_3O_4; red circle = condition for synthesizing the Fe_4O_5 starting material. Open symbols are the data from **a**. The Fe_5O_6 + h-Fe_3O_4 region is supposed to exist, although not observed in this study. The dark gray area is the region where Woodland et al. (2012) reported the breakdown of Fe_3O_4 into Fe_2O_3 + Fe_4O_5. The light gray area indicates the conditions at which Fe_4O_5 was synthesized by Lavina et al. (2011). The dashed line is based on Myhill et al. (2016). The chain curve shows the melting curve of FeO (Fischer and Campbell 2010), which can be a guide for melting temperatures of Fe_5O_6 and Fe_4O_5. Error bars are smaller than symbols where they are not shown. (Color online.)

Compression curve of Fe_4O_5

We obtained the volume of Fe_4O_5 at 300 K in a wide pressure range from 8 to 61 GPa (Table S1 and Fig. S3 in the Supplemental Information[1]). A large volume reduction (~3%) was observed at 50 GPa (Fig. 3). Since the volumes of Fe_4O_5 above 50 GPa are too small to be fitted by a single compression curve together with the lower pressure data, we fit a third-order Birch-Murnaghan equation of state (EoS) to these pressure-volume data up to 47 GPa, which gives bulk modulus at 1 bar of K_0 = 201(7) GPa and its pressure derivative, K' = 3.1(5) using V_0 = 357.1 Å^3 at 1 bar from Lavina et al. (2011). When we instead fit a second-order BM EoS, we obtained K_0 = 188(2) GPa, consistent with the K_0 = 185.7 GPa reported by Lavina et al. (2011) based on their data up to 28 GPa.

DISCUSSION

While only three iron oxides, FeO wüstite, Fe_3O_4 magnetite, and Fe_2O_3 hematite, are found at 1 bar, recent high-pressure

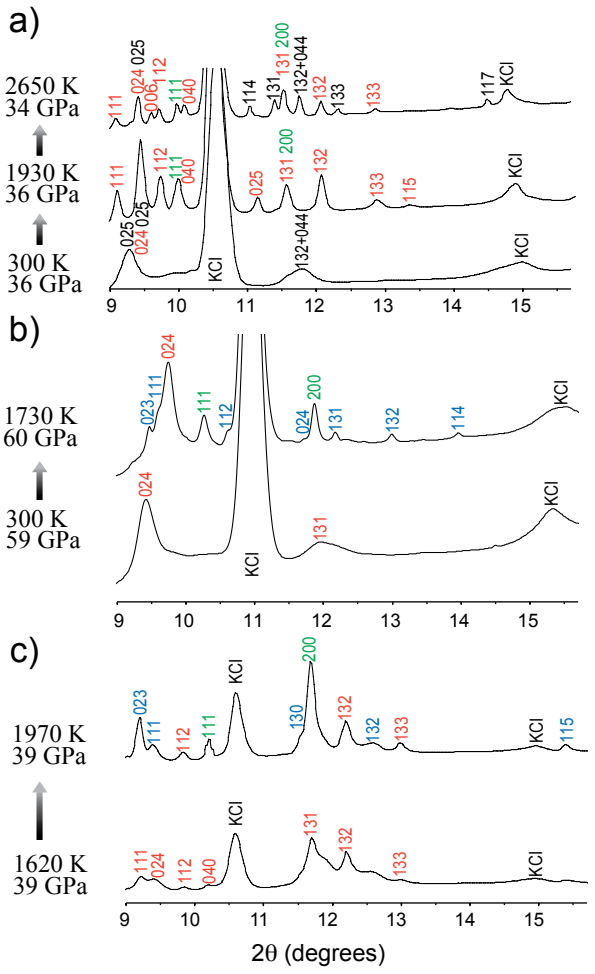

FIGURE 2. Changes in XRD patterns (**a** and **b**) in run 8 and (**c**) in run 12, using the Fe_5O_6 and Fe_4O_5 starting materials, respectively. The wavelength of the incident X-ray beam was 0.4141 Å for the former and 0.4150 Å for the latter. The color of labels: black = Fe_5O_6, red = Fe_4O_5, blue = h-Fe_3O_4, and green = FeO. Peak positions moved to some extent upon heating because of the release of large deviatoric stress at 300 K. See text for further details. (Color online.)

experiments report a rich variety of intermediate compounds between FeO and Fe_3O_4 above ~10 GPa. They include not only Fe_4O_5 and Fe_5O_6, which were directly examined in this study, but also Fe_9O_{11} (Ishii et al. 2018) and Fe_7O_9 (Sinmyo et al. 2016). In the Earth's interior, these iron oxides may be formed in Fe^{3+}-bearing oxidizing materials such as subducted banded iron formations (BIFs) and play important roles in oxidation/reduction reactions in the presence of fluids. This study demonstrates that FeO coexists with Fe_3O_4 above 38 GPa and 1950 K, which is the invariant triple point where FeO, Fe_5O_6, Fe_4O_5, and h-Fe_3O_4 coexist in the two-component system (Fig. 1). These findings indicate that any intermediate compounds between FeO and Fe_3O_4 cannot form beyond that point. Therefore, the roles of Fe_5O_6, Fe_9O_{11}, Fe_4O_5, and Fe_7O_9 in oxidation/reduction reactions are limited to *P-T* conditions of the deep upper mantle to the shallow lower mantle.

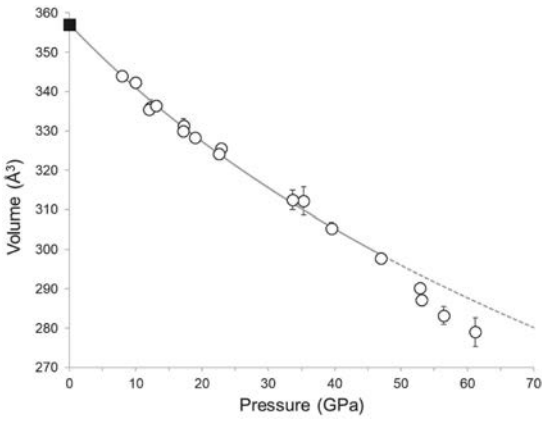

FIGURE 3. Compression curve of Fe_4O_5. The volume at 1 bar is from Lavina et al. (2011). Error bars are smaller than symbols where they are not shown. The solid gray curve is the fit by third-order Birch-Murnaghan equation of state based on data up to 47 GPa that yields K_0 = 201(7) GPa and K' = 3.1(5). A ~3% volume reduction is found above 50 GPa.

Our experiments show that Fe_4O_5 undergoes a distinct volume contraction at around 50 GPa (Fig. 3). This mirrors the significant volume reduction that was previously reported to occur in h-Fe_3O_4 at ~50 GPa (Ricolleau and Fei 2016), which is caused by the high-spin to low-spin transition of octahedral Fe^{3+} (Greenberg et al. 2017). The structural similarity between Fe_4O_5 and h-Fe_3O_4 suggests that the observed volume change in Fe_4O_5 might also be attributed to the spin transition of Fe^{3+}.

IMPLICATIONS

The origins of superdeep diamonds may be related to carbonaceous melts, C-H-O fluids, or Fe-rich metallic melts in a deep mantle (Shirey et al. 2013; Smith et al. 2016). Magnesiowüstite (Mg,Fe)O found as inclusions in such superdeep diamonds is associated with Fe^{3+}-rich phases as exsolution lamella or clusters (Kaminsky et al. 2015). Their bulk composition suggests that these inclusions (magnesiowüstite + Fe^{3+}-rich phases) are relics of high-pressure iron oxides such as Fe_4O_5 and Fe_5O_6. Myhill et al. (2016) reported that the EMOD buffer line is in the Fe_5O_6 stability field and thus Fe_5O_6 can coexist with diamond, while Fe_4O_5 can co-occur only with carbonate. Accordingly, such diamond inclusions (magnesiowüstite + Fe^{3+}-rich phases) could be relics of the decomposition of Fe_5O_6 that, as shown by this study, has a stability field limited to high *P-T* conditions (>10 GPa and >1500 K) (Fig. 1a). This stability field is close to the conditions along normal mantle geotherm and the solidus of carbonated mantle rocks (Dasgupta 2013). The host diamonds may, therefore, have a genetic link with CO_2-rich partial melts in the deep upper mantle and below.

ACKNOWLEDGMENTS AND FUNDING

Synchrotron XRD data were collected at BL10XU, SPring-8 (proposal no. 2017B0072, 2018A0072, and 2018B0072). We thank Y. Kuwayama for his help in the measurements. Comments provided from three anonymous reviewers helped improve the manuscript.

REFERENCES CITED

Brown, J.M. (1999) The NaCl pressure standard. Journal of Applied Physics, 86, 5801–5808.

Dasgupta, R. (2013) Ingassing, storage, and outgassing of terrestrial carbon through geologic time. Reviews in Mineralogy and Geochemistry, 75, 183–229.

Dewaele, A., Belonoshko, A.B., Garbarino, G., Occelli, F., Bouvier, P., Hanfland, M., and Mezouar, M. (2012) High-pressure–high-temperature equation of state of KCl and KBr. Physical Review B, 85, 214105.

Fischer, R.A., and Campbell, A.J. (2010) High-pressure melting of wüstite. American Mineralogist, 95, 1473–1477.

Greenberg, E., Xu, W.M., Nikolaevsky, M., Bykova, E., Garbarino, G., Glazyrin, K., Merkel, D.G., Dubrovinsky, L., Pasternak, M.P., and Rozenberg, G.K. (2017) High-pressure magnetic, electronic, and structural properties of $M Fe_2O_4$ (M = Mg,Zn,Fe) ferric spinels. Physical Review B, 95, 195150.

Ishii, T., Shi, L., Huang, R., Tsujino, N., Druzhbin, D., Myhill, R., Li, Y., Wang, L., Yamamoto, T., Miyajima, N., and others. (2016) Generation of pressures over 40 GPa using Kawai-type multi-anvil press with tungsten carbide anvils. Review of Scientific Instruments, 87, 024501.

Ishii, T., Uenver-Thiele, L., Woodland, A.B., Alig, E., and Boffa Ballaran, T. (2018) Synthesis and crystal structure of Mg-bearing Fe_9O_{11}: New insight in the complexity of Fe-Mg oxides at conditions of the deep upper mantle. American Mineralogist, 103, 1873–1876.

Kaminsky, F.V., Ryabchikov, I.D., McCammon, C.A., Longo, M., Abakumov, A.M., Turner, S., and Heidari, H. (2015) Oxidation potential in the Earth's lower mantle as recorded by ferropericlase inclusions in diamond. Earth and Planetary Science Letters, 417, 49–56.

Lavina, B., and Meng, Y. (2015) Unraveling the complexity of iron oxides at high pressure and temperature: Synthesis of Fe_5O_6. Science Advances, 1, e1400260.

Lavina, B., Dera, P., Kim, E., Meng, Y., Downs, R.T., Weck, P.F., Sutton, S.R., and Zhao, Y. (2011) Discovery of the recoverable high-pressure iron oxide Fe_4O_5. Proceedings of the National Academy of Sciences, 108, 17,281–17,285.

Myhill, R., Ojwang, D.O., Ziberna, L., Frost, D.J., Ballaran, T.B., and Miyajima, N. (2016) On the P-T-f_{O_2} stability of Fe_4O_5, Fe_5O_6 and Fe_4O_5-rich solid solutions. Contributions to Mineralogy and Petrology, 171, 51.

Ozawa, H., Hirose, K., Yonemitsu, K., and Ohishi, Y. (2016) High-pressure melting experiments on Fe–Si alloys and implications for silicon as a light element in the core. Earth and Planetary Science Letters, 456, 47–54.

Pigott, J.S., Ditmer, D.A., Fischer, R.A., Reaman, D.M., Hrubiak, R., Meng, Y., Davis, R.J., and Panero, W.R. (2015) High-pressure, high-temperature equations of state using nanofabricated controlled-geometry Ni/SiO_2/Ni double hot-plate samples. Geophysical Research Letters, 42, 10,239–10,247.

Ricolleau, A., and Fei, Y. (2016) Equation of state of the high-pressure Fe_3O_4 phase and a new structural transition at 70 GPa. American Mineralogist, 101, 719–725.

Shirey, S.B., Cartigny, P., Frost, D.J., Keshav, S., Nestola, F., Nimis, P., Pearson, D.G., Sobolev, N.V., and Walter, M.J. (2013) Diamonds and the geology of mantle carbon. Reviews in Mineralogy and Geochemistry, 75, 355–421.

Sinmyo, R., Bykova, E., Ovsyannikov, S.V., McCammon, C., Kupenko, I., Ismailova, L., and Dubrovinsky, L. (2016) Discovery of Fe_7O_9: A new iron oxide with a complex monoclinic structure. Scientific Reports, 6, 32852.

Smith, E.M., Shirey, S.B., Nestola, F., Bullock, E.S., Wang, J., Richardson, S.H., and Wang, W. (2016) Large gem diamonds from metallic liquid in Earth's deep mantle. Science, 354, 1403–1405.

Ueda, Y., Matsui, M., Yokoyama, A., Tange, Y., and Funakoshi, K. (2008) Temperature-pressure-volume equation of state of the B2 phase of sodium chloride. Journal of Applied Physics, 103, 113513.

Woodland, A.B., Frost, D.J., Trots, D.M., Klimm, K., and Mezouar, M. (2012) In situ observation of the breakdown of magnetite (Fe_3O_4) to Fe_4O_5 and hematite at high pressures and temperatures. American Mineralogist, 97, 1808–1811.

Manuscript received May 3, 2019
Manuscript accepted June 4, 2019
Manuscript handled by Ian Swainson

Endnote:

[1]Deposit item AM-19-97097, Supplemental Material. Deposit items are free to all readers and found on the MSA website, via the specific issue's Table of Contents (go to http://www.minsocam.org/MSA/AmMin/TOC/2019/Sep2019_data/Sep2019_data.html).